Supporting Information

Light and Complex 3D MoS_2/Graphene Heterostructures as a Highly Efficient Catalyst for the Hydrogen Evolution Reaction

Jonah Teich,[*†] Ravit Dvir,[*†] Alex Henning,[*§] Eliran Hamo,[†] Michael J. Moody,[§] Titel Jurca,[‡] Hagai Cohen,[⊥] Tobin J. Marks,[‡§] Brian A. Rosen,[†] Lincoln J. Lauhon[§] and Ariel Ismach[†#]

† Department of Materials Science and Engineering, Tel Aviv University, Ramat Aviv, Tel Aviv, 6997801, Israel
§ Department of Materials Science and Engineering, Northwestern University, Evanston, IL 60208, United States
‡ Department of Chemistry, Northwestern University, Evanston, IL 60208, United States
⊥ Weizmann Inst Science, Department of Chemical Research Support, IL-76100 Rehovot, Israel
* These authors contributed equally to this work
# E-mail: aismach@tauex.tau.ac.il

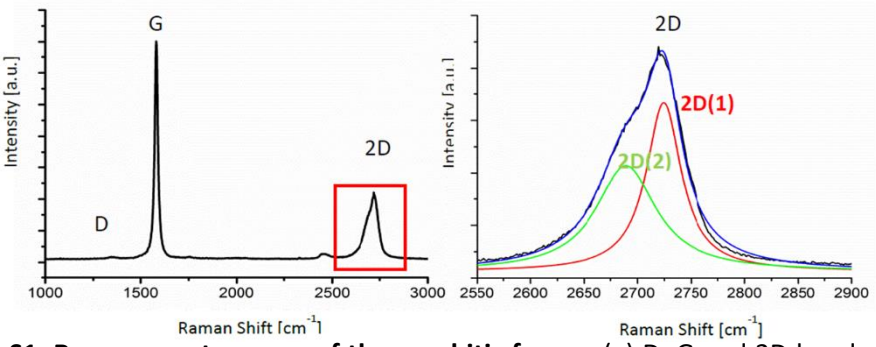

Figure S1: Raman spectroscopy of the graphitic foams. (a) D, G and 2D band positions. (b) Fitting of the 2D peak shows a characteristic AB-stacking graphitic mode.

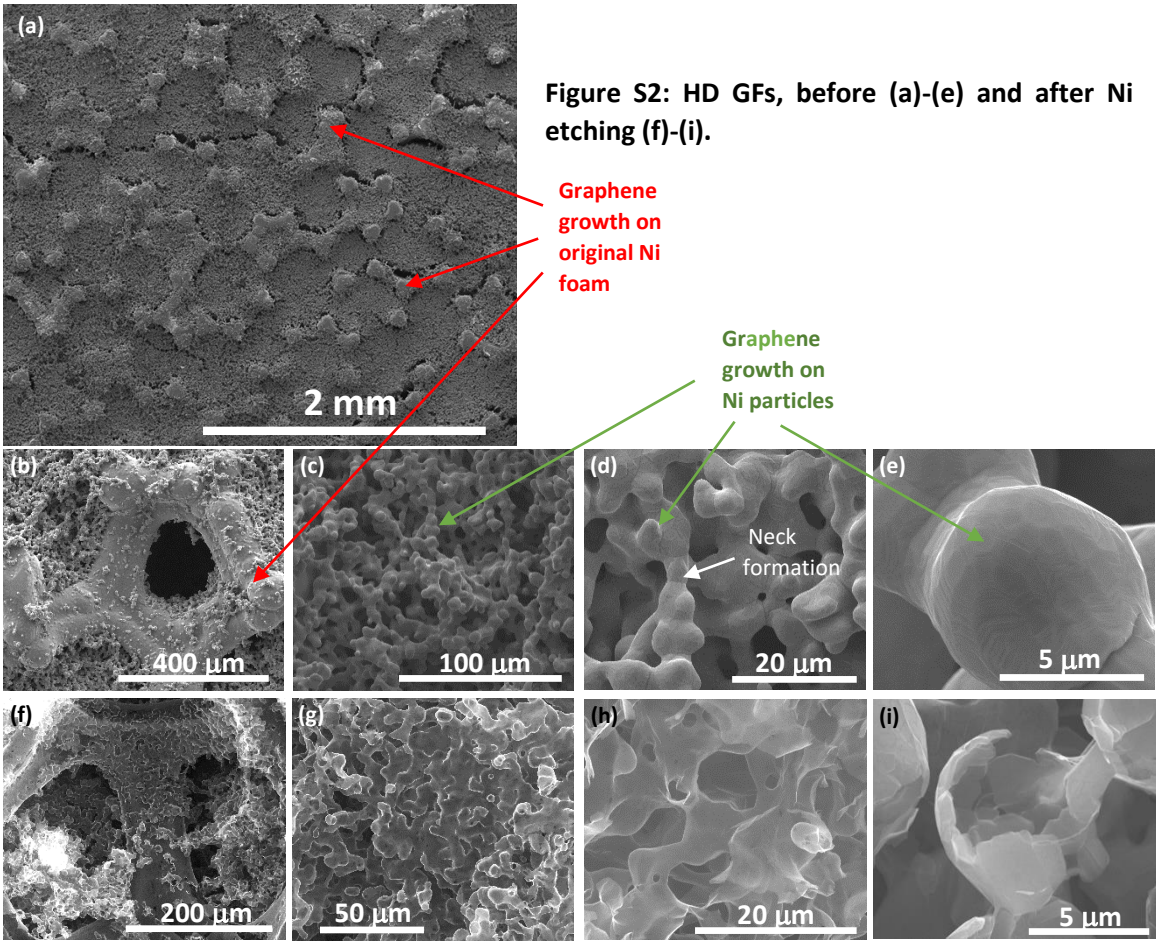

Figure S2: HD GFs, before (a)-(e) and after Ni etching (f)-(i).

Table S1: Resistivity of the different graphene foams

Sample	*Resistivity [Ωm]*
LD GF	0.053
HD GF	0.027

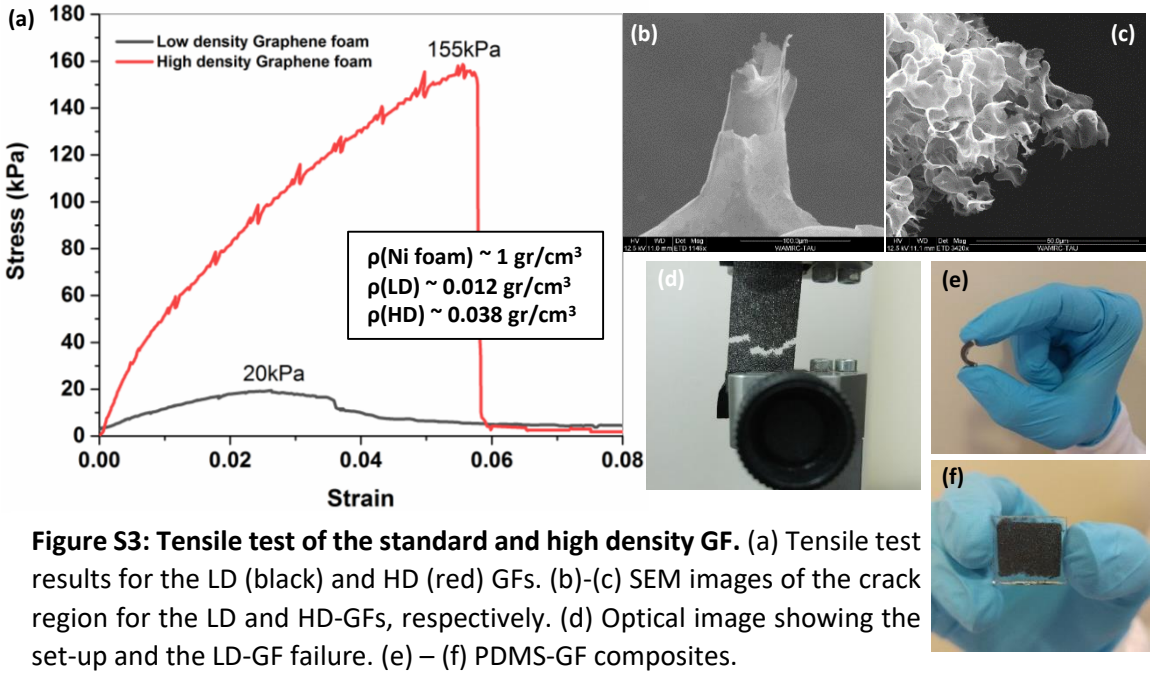

Figure S3: Tensile test of the standard and high density GF. (a) Tensile test results for the LD (black) and HD (red) GFs. (b)-(c) SEM images of the crack region for the LD and HD-GFs, respectively. (d) Optical image showing the set-up and the LD-GF failure. (e) – (f) PDMS-GF composites.

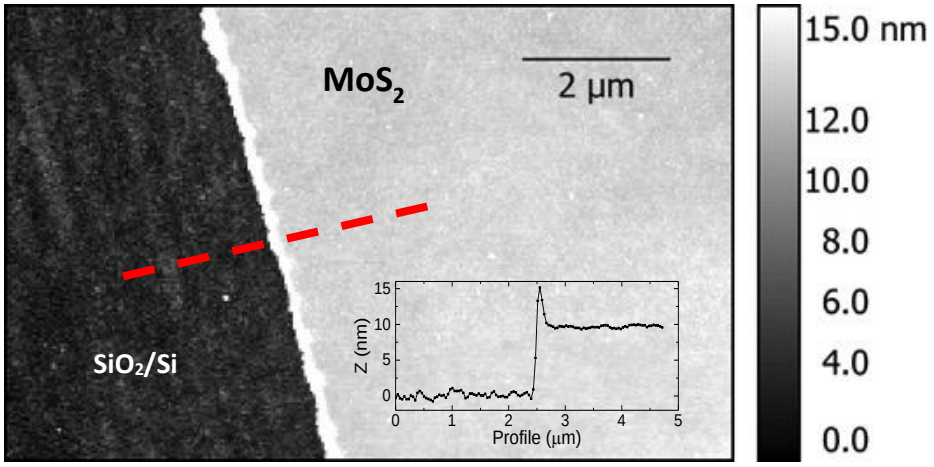

Figure S4: Atomic force microscopy of the 10 nm (100 cycles) MoS_2 film. The inset shows the cross section along the red line.

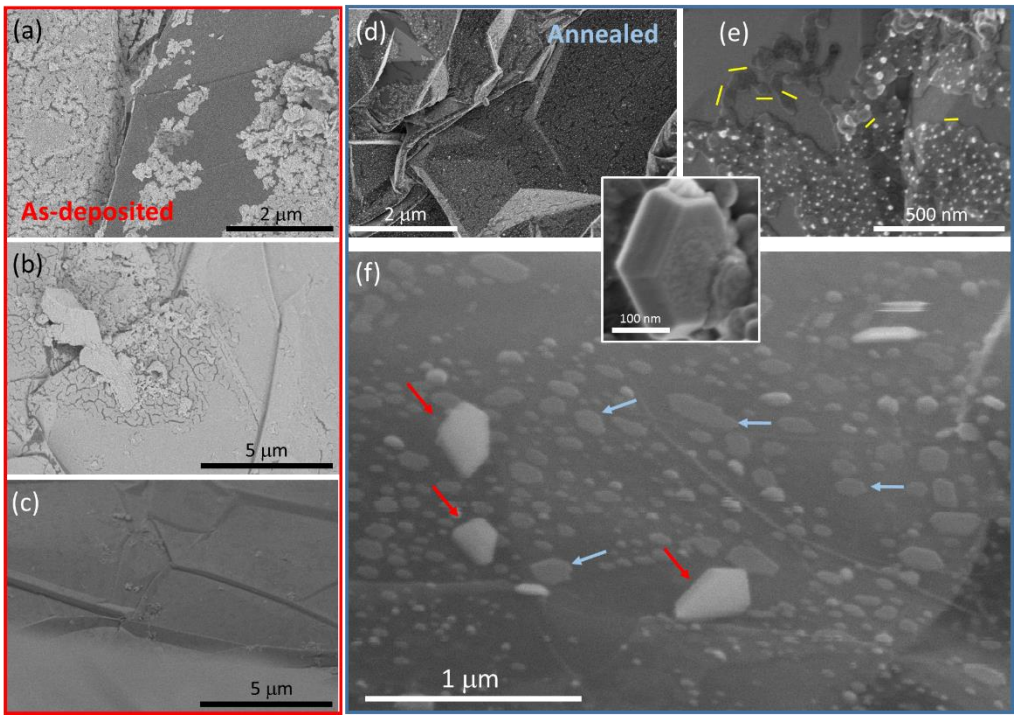

Figure S5: MoS_2 film Morphology before and after annealing: (a) BSE image showing the MoS_2 (bright) and the GF (dark) at the foam edge and (b) in an inner area of the foam. (c) SE image showing a smooth continuous film as deposited. (d)-(f) SEM images showing the formation of 100-400 nm crystals after annealing at 800 °C. The vast majority laying parallel to the GF substrate, as shown in (e) by the yellow lines emphasizing the facets and the blue arrows in (f). The red arrows in (f) point to vertical hexagonal crystals, as the one shown in high magnification in the inset.

For comparison, LD- and HD-GFs were coated with MoS_2 using wet chemistry approaches. In this scheme, ~50 mg Ammonium tetrathiomolybdate ($(NH_4)_2MoS_4$) were dissolved in 30 ml N,N-dimethylformamide (DMF) by ultrasonication. The solution was drop casted (5-10 10µl drops) or the GF was immersed for few minutes in the solution and dried.

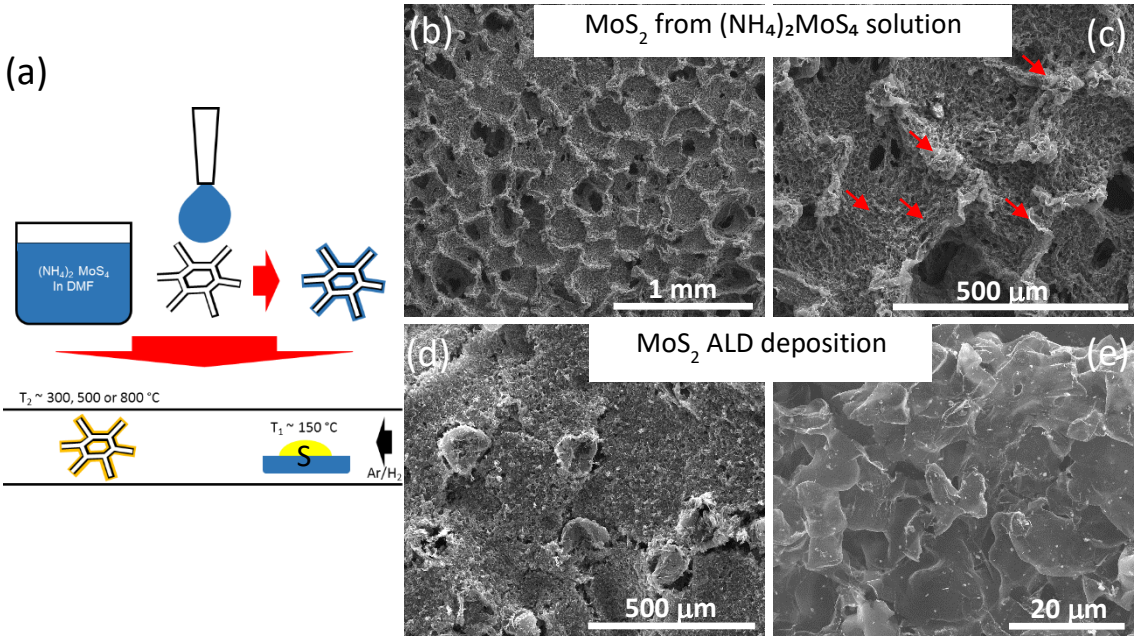

Figure S6: Comparison between liquid-phase and ALD – derived MoS_2 coatings: (a) Schematic representation of the liquid-phase methodology. (b)-(c) SEM images showing the morphology of the HD-800 sample prepared via liquid-phase. (d)-(e) HD-800 sample prepared via ALD, which preserves the HD-GF morphology.

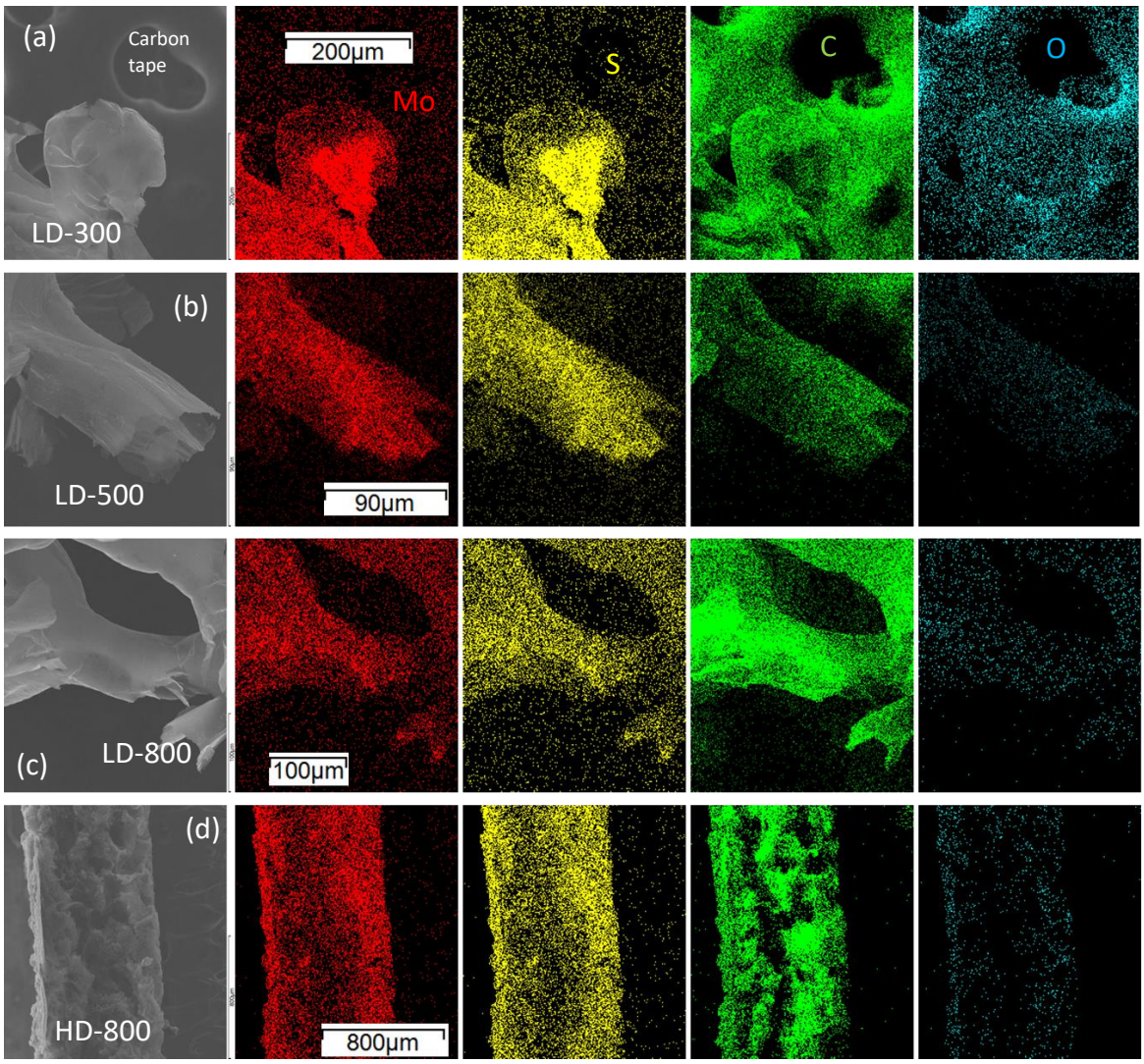

Figure S7: EDS mapping MoS_2/GFS: (a) LD-300, (b) LD-500, (c) LD-800 and (d) HD-800. From left to right, SEM image of the mapping area, mapping of the Mo (red), S (yellow), C (green) and O (light blue).

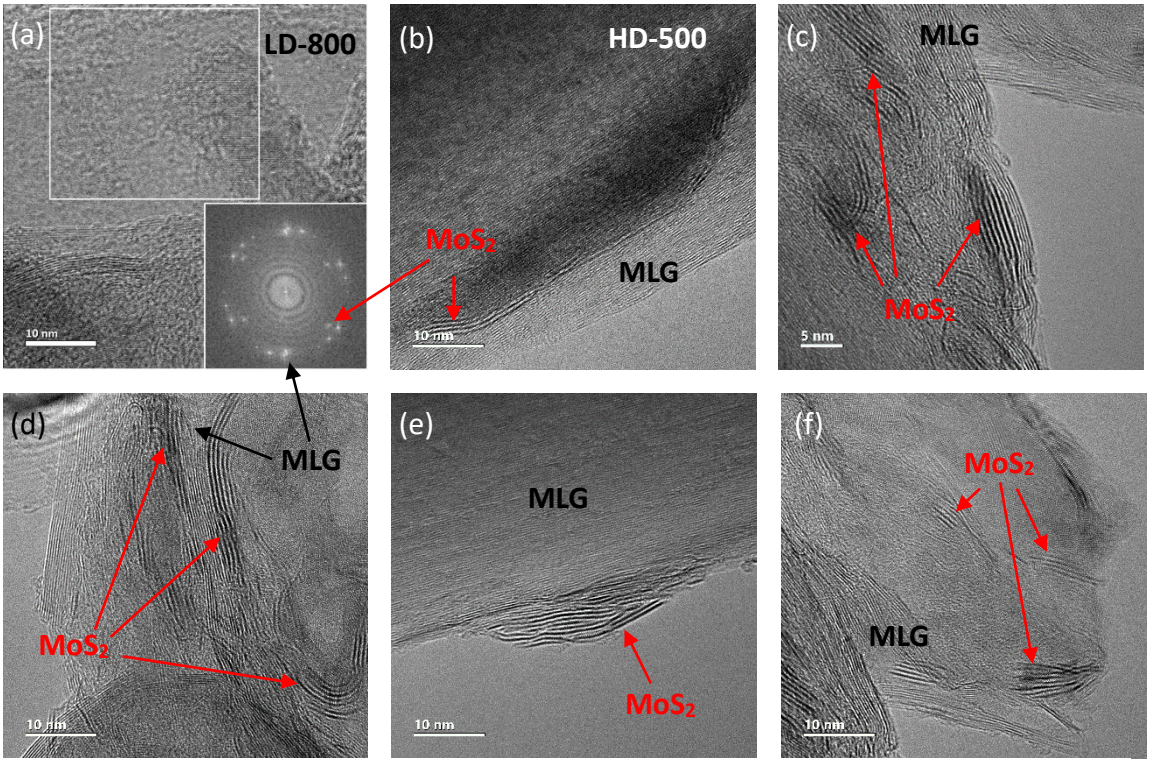

Figure S8: Additional HRTEM images of the MoS2/GFs heterostructures.

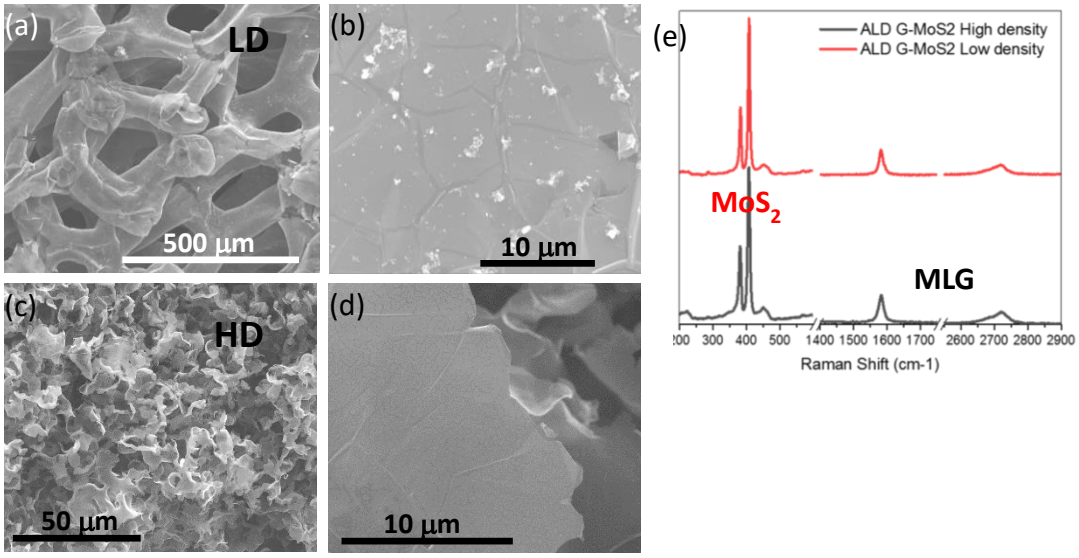

Figure S9: Additional SEM and Raman data. (a)-(b) LD-800, (c)-(d) HD-800. (e) The respective Raman spectra showing the two phases, MoS2 and MLG characteristic peaks.

Table S2: Raman spectroscopy characterization of the 3D MoS_2/GF heterostructures.

Sample	*FWHM (E_{2g}) [cm^{-1}]*	*FWHM (A_{1g}) [cm^{-1}]*	*$I(A_{1g})/I(G)$*
500-MoS_2/GF	14.2	12.5	0.68
800-MoS_2/GF	9.7	9.2	3.32

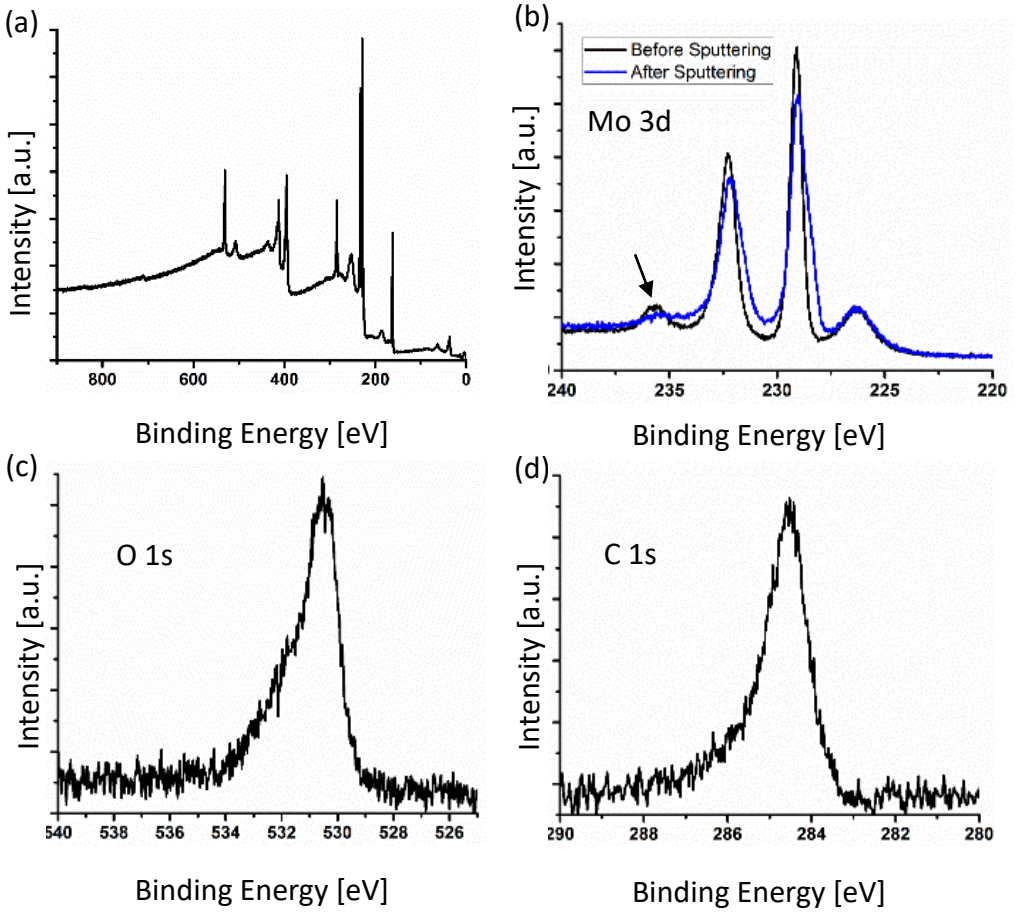

Figure S10: XPS characterization: (a) Survey, (b) Mo 3d before and after sputtering showing the reduction of the MoO_3 contribution (black arrow), (c) O 1s and (d) C 1s spectra.

Electrochemical surface area determination was conducted using double layer capacitance at room temperature in the same three-electrode glass cell using a Bio-Logic VSP-300 potentiostat. This method based on double layer capacity voltammetric curves, which recorded in the mere double layer region at various scan rates. Then, a plot of the current in the middle of the potential window vs. scan rate is constructed. Under the condition, where the double layer charging is the only process occurring in that potential range, this plot is a straight line, whose slope gives the value of double layer differential capacity. The surface area can be calculated by referring the obtained capacity to the reference value of capacity per the unit area (C_{ref}):

$ECSA = C / C_{ref}$

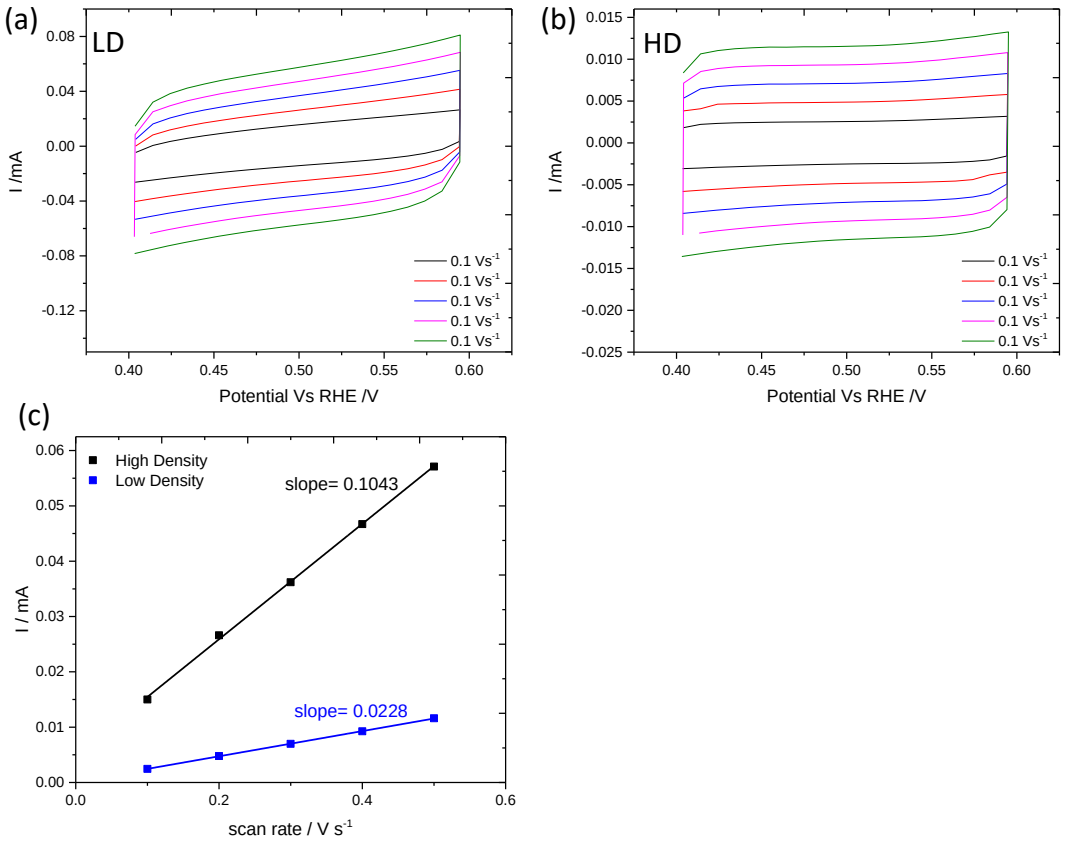

Figure S11: Electrochemical Surface Area (ESCA) measurements: (a) –(b) Double layer charging currents recorded with various scan rates in 0.5 M H_2SO_4 (298 K) for the LD- (a), and HD-GFs (b). (c) Double layer charging current at potential of 0.50 vs. RHE on scan rate for a polycrystalline Pt electrode in 0.5 M H_2SO_4.

Table S3- Comparison of HER catalytic performance

Catalyst	Morphology	3D compatible	η(mV)@*j*= -10mA/cm^2	Tafel slope (mV/dec)	Ref.
ALD-MoS_2/GF	***Thin film coated GF***	***Y (ALD)***	***180***	***47***	***This work***
ALD-MoS_2	Thin films	Y (ALD)	~225	61	[1]
ALD-MoS_2	Thin films	Y (ALD)	~222	57	[2]
ALD-MoS_2	Thin films	Y (ALD)	>227 @ j=-5mA/cm^2	47	[3]
Amorphous MoS_2	Thin films	M (wet-chem)	~225	40	[4]
MoS_2/Graphene/Ni foam	nanosheets	M (wet-chem)	140	42	[5]
defect-rich MoS_2	nanosheets	M (wet-chem)	180	50	[6]
Oxygen-incorporated MoS_2	nanosheets	M (wet-chem)	180	55	[7]
MoS_2	film	M (vapor-phase)	170	60	[8]
mesoporous MoS_2	nanosized	Y (electrodeposition + sulfurization)	~250	50	[9]
metallic MoS_2	nanosheets	M (wet-chem)	187	43	[10]
MoSx- Graphene	nanoparticles	M (wet-chem)	~180	43	[11]
MoS_2/graphite paper	flakes	M (vapor-phase)	350	54	[12]
MoS_2/carbon cloth	nanosheets	M (wet-chem)	150	50	[13]
MoS_2/Graphene/Ni foam	nanoparticles	M (wet-chem)	160	43	[14]

Superaerophobic MoS_2 film	nanosize	M (wet-chem)	200	51	[15]
Amorphous MoS_x	Film	N (PVD)	180	45	[16]
Etched MoS_2 flakes	Isolated flakes	N	540	138	[17]
Amorphous MoS_2	Nanosized Amorphous MoSx	N	145	40	[18]
Porous MoS_2	~100nm pores	M (wet-chem)	210	113	[19]
Li-Intercalated VA-MoS_2	Li-VA MoS_2 films	M (vapor-phase) + electrochemical intercalation	210	43-47	[20]
VA-MoS_2/graphene	MoS_2/ graphene film	M (vapor-phase)	420	54	[21]

Y- Yes, compatible, M-moderate, N – not compatible.

Most of the wet-chemical approaches are labeled with "M" for a moderate compatibility with 3D porous structures due the inducement of morphological changes in small pore sizes, as shown in Figures S5 (b) and (c).

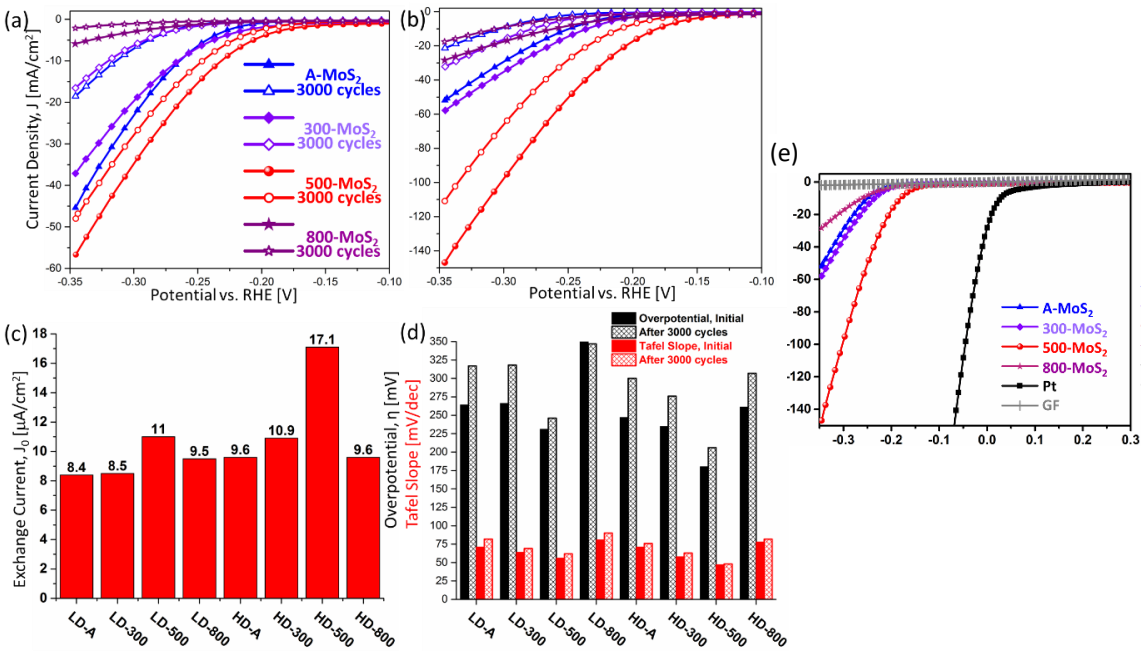

Figure S12: HER stability measurements: (a)-(b) Polarization curves for the LD, (a), and HD, (b), foams at the initial and after 3000 cycles. (c) Exchange currents for the different MoS2/GFs. (d) Overpotential and Tafel slopes for the different foams at the initial and after 3000 cycles. (e) Polarization curves for the HD foams with the pristine GF data, in grey, confirming it is not active towards HER.

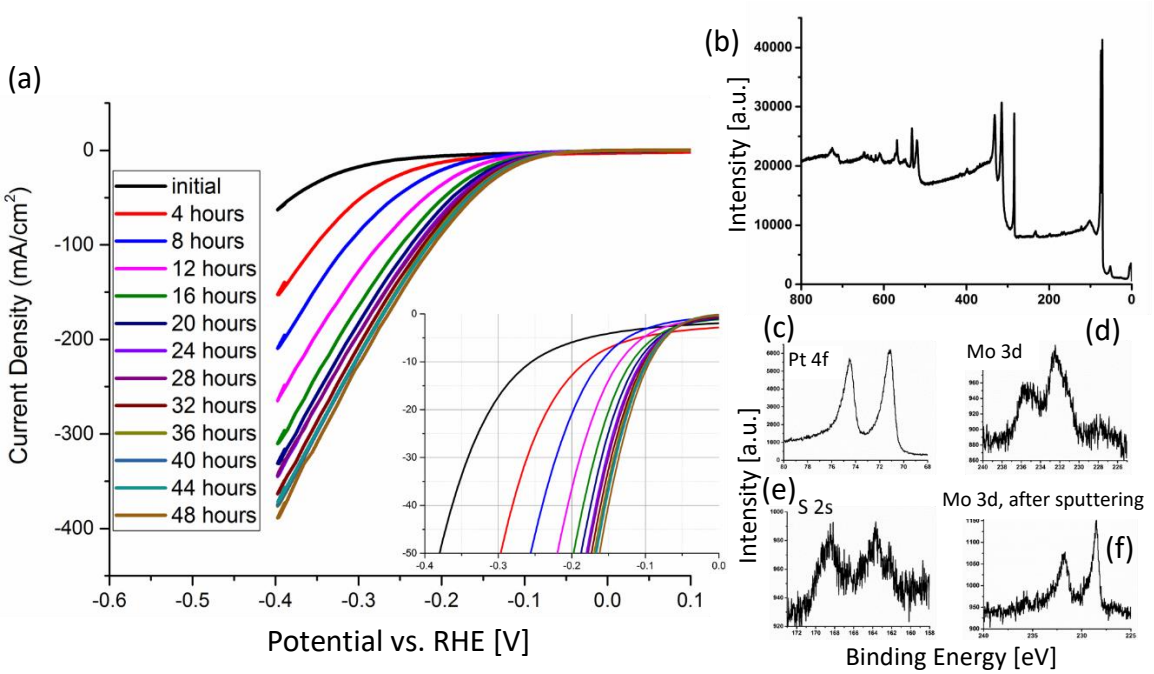

Figure S13: Effect of Pt as a counter electrode: (a) Polarization curves obtained with a Pt as a counter electrode, showing that the catalytic performance is increased with time, suggesting there is Pt deposition on the working electrode. (b)-(f) XPS characterization of such working electrode after HER measurements. Survey, (b), Pt 4f, (c), Mo 3d, (d), S 2p, (e) and Mo 3d after sputtering to clean the Pt on the surface, (f).

References

[1] T.A. Ho, C. Bae, S. Lee, M. Kim, J.M. Montero-Moreno, J.H. Park, H. Shin, Edge-On MoS2 Thin Films by Atomic Layer Deposition for Understanding the Interplay between the Active Area and Hydrogen Evolution Reaction, Chemistry of Materials, 29 (2017) 7604-7614.

[2] D.H. Kwon, Z. Jin, S. Shin, W.-S. Lee, Y.-S. Min, A comprehensive study on atomic layer deposition of molybdenum sulfide for electrochemical hydrogen evolution, Nanoscale, 8 (2016) 7180-7188.

[3] S. Shin, Z. Jin, D.H. Kwon, R. Bose, Y.-S. Min, High Turnover Frequency of Hydrogen Evolution Reaction on Amorphous MoS2 Thin Film Directly Grown by Atomic Layer Deposition, Langmuir, 31 (2015) 1196-1202.

[4] D. Merki, S. Fierro, H. Vrubel, X. Hu, Amorphous molybdenum sulfide films as catalysts for electrochemical hydrogen production in water, Chemical Science, 2 (2011) 1262-1267.

[5] P. Zhu, Y. Chen, Y. Zhou, Z. Yang, D. Wu, X. Xiong, F. Ouyang, Defect-rich MoS2 nanosheets vertically grown on graphene-protected Ni foams for high efficient electrocatalytic hydrogen evolution, International Journal of Hydrogen Energy, 43 (2018) 14087-14095.

[6] J.F. Xie, H. Zhang, S. Li, R.X. Wang, X. Sun, M. Zhou, J.F. Zhou, X.W. Lou, Y. Xie, Defect-Rich MoS2 Ultrathin Nanosheets with Additional Active Edge Sites for Enhanced Electrocatalytic Hydrogen Evolution, Advanced Materials, 25 (2013) 5807-+.

[7] J. Xie, J. Zhang, S. Li, F. Grote, X. Zhang, H. Zhang, R. Wang, Y. Lei, B. Pan, Y. Xie, Controllable Disorder Engineering in Oxygen-Incorporated MoS2 Ultrathin Nanosheets for Efficient Hydrogen Evolution, Journal of the American Chemical Society, 135 (2013) 17881-17888.
[8] H. Li, C. Tsai, A.L. Koh, L. Cai, A.W. Contryman, A.H. Fragapane, J. Zhao, H.S. Han, H.C. Manoharan, F. Abild-Pedersen, J.K. Norskov, X. Zheng, Activating and optimizing MoS2 basal planes for hydrogen evolution through the formation of strained sulphur vacancies, Nature Materials, 15 (2016) 48-+.
[9] J. Kibsgaard, Z. Chen, B.N. Reinecke, T.F. Jaramillo, Engineering the surface structure of MoS2 to preferentially expose active edge sites for electrocatalysis, Nature Materials, 11 (2012) 963-969.
[10] M.A. Lukowski, A.S. Daniel, F. Meng, A. Forticaux, L. Li, S. Jin, Enhanced Hydrogen Evolution Catalysis from Chemically Exfoliated Metallic MoS2 Nanosheets, Journal of the American Chemical Society, 135 (2013) 10274-10277.
[11] Z. Pu, Q. Liu, A.M. Asiri, A.Y. Obaid, X. Sun, Graphene film-confined molybdenum sulfide nanoparticles: Facile one-step electrodeposition preparation and application as a highly active hydrogen evolution reaction electrocatalyst, Journal of Power Sources, 263 (2014) 181-185.
[12] G.R. Bhimanapati, T. Hankins, Y. Lei, R.A. Vilá, I. Fuller, M. Terrones, J.A. Robinson, Growth and Tunable Surface Wettability of Vertical MoS2 Layers for Improved Hydrogen Evolution Reactions, ACS Applied Materials & Interfaces, 8 (2016) 22190-22195.
[13] Y. Yan, B. Xia, N. Li, Z. Xu, A. Fisher, X. Wang, Vertically oriented MoS2 and WS2 nanosheets directly grown on carbon cloth as efficient and stable 3-dimensional hydrogen-evolving cathodes, Journal of Materials Chemistry A, 3 (2015) 131-135.
[14] Y.-H. Chang, C.-T. Lin, T.-Y. Chen, C.-L. Hsu, Y.-H. Lee, W. Zhang, K.-H. Wei, L.-J. Li, Highly Efficient Electrocatalytic Hydrogen Production by MoSx Grown on Graphene-Protected 3D Ni Foams, Advanced Materials, 25 (2013) 756-760.
[15] Z.Y. Lu, W. Zhu, X.Y. Yu, H.C. Zhang, Y.J. Li, X.M. Sun, X.W. Wang, H. Wang, J.M. Wang, J. Luo, X.D. Lei, L. Jiang, Ultrahigh Hydrogen Evolution Performance of Under-Water "Superaerophobic" MoS2 Nanostructured Electrodes, Advanced Materials, 26 (2014) 2683-2687.
[16] F. Xi, P. Bogdanoff, K. Harbauer, P. Plate, C. Hoelm, J. Rappich, B. Wang, X. Han, R. van de Krol, S. Fiechter, Structural Transformation Identification of Sputtered Amorphous MoSX as an Efficient Hydrogen-Evolving Catalyst during Electrochemical Activation, Acs Catalysis, 9 (2019) 2368-2380.
[17] P. Zhang, H. Xiang, L. Tao, H. Dong, Y. Zhou, T.S. Hu, X. Chen, S. Liu, S. Wang, S. Garaj, Chemically activated MoS2 for efficient hydrogen production, Nano Energy, 57 (2019) 535-541.
[18] B. Li, L. Jiang, X. Li, Z. Cheng, P. Ran, P. Zuo, L. Qu, J. Zhang, Y. Lu, Controllable Synthesis of Nanosized Amorphous MoSx Using Temporally Shaped Femtosecond Laser for Highly Efficient Electrochemical Hydrogen Production, Advanced Functional Materials, 29 (2019).
[19] S.R. Kadam, U.V. Kawade, R. Bar-Ziv, S.W. Gosavi, M. Bar-Sadan, B.B. Kale, Porous MoS2 Framework and Its Functionality for Electrochemical Hydrogen Evolution Reaction and Lithium Ion Batteries, ACS Applied Energy Materials, 2 (2019) 5900-5908.
[20] H. Wang, Z. Lu, S. Xu, D. Kong, J.J. Cha, G. Zheng, P.-C. Hsu, K. Yan, D. Bradshaw, F.B. Prinz, Y. Cui, Electrochemical tuning of vertically aligned MoS₂ nanofilms and its application in improving hydrogen evolution reaction, Proceedings of the National Academy of Sciences, 110 (2013) 19701-19706.
[21] P. Gnanasekar, D. Periyanagounder, J. Kulandaivel, Vertically aligned MoS2 nanosheets on graphene for highly stable electrocatalytic hydrogen evolution reactions, Nanoscale, 11 (2019) 2439-2446.